

# Existence and Uniqueness of Weak Solutions and Error Analysis of the Galerkin Finite Element Method for Time-Dependent Convective Nanofluid Poiseuille Flow Problems

Andrew O. McCartney<sup>1</sup>, Victor M. Job<sup>2,\*</sup>

<sup>1</sup> Department of Mathematics, The University of the West Indies, Mona Campus, Jamaica, W.I.

<sup>2</sup> Department of Mathematics, The University of the West Indies, Mona Campus, Jamaica, W.I.

Received: June 29, 2023

Accepted : Feb. 4, 2024

**Abstract:** A finite element analysis of the plane Poiseuille nanofluid flow and heat transfer based on the time-dependent Buongiorno model equations is performed. A suitable weak formulation of the sequentially-linearized governing equations is first constructed. Then, the spatial discretization of the weak form is done using the Galerkin finite element formulation, while a Backward-Euler finite difference scheme is used for the temporal discretization. Existence, uniqueness, and stability of the weak, semi-discrete and fully-discrete forms are discussed. Furthermore,  $L^2$ -error estimates for the semi-discrete and fully-discrete forms are obtained. Moreover, numerical computations are performed to verify the theoretical results and estimate the rate of convergence.

**Keywords:** Buongiorno model; Finite element analysis; Galerkin formulation;  $L^2$ -error estimates; Poiseuille flow.

**2010 Mathematics Subject Classification.** 65M60; 76M10.

## 1 Introduction

The finite element method was first formally introduced by Turner et al. [1] as a means of solving particular differential equation problems in structural mechanics. Its most notable feature involves the breaking up of any given domain into a finite set of simpler domains, which are each known as a finite element. This is a key advantage over numerical techniques such as the finite difference method and allows it to be a powerful tool in solving many complex engineering problems. The beauty of the method is that the solution of the problem over each finite element is found and then connected to form an approximation of the solution over the entire domain. Initially, the finite element method was built for the still highly-popular Galerkin formulation; however, more techniques have been developed such as the mixed finite element method, stabilized finite element methods, and spectral element method. While initially conceived for structural mechanics, the finite element method has since been found invaluable in areas such as computer animation, biomedical sciences, and fluid dynamics.

Over decades, the finite element analysis of parabolic problems has long been a focal point of research due to these problems playing significant roles in areas such as physics, chemistry, and financial mathematics. Wheeler [2] performed finite element analysis on some non-linear parabolic equations. Separate cases of Dirichlet and Neumann boundary conditions were analyzed for the corresponding initial boundary value problem.  $L^2$ -error estimates for both the semi-discrete and fully-discrete forms (based on the Forward-Euler and Crank-Nicolson schemes) were obtained in all examined cases. Weng, Feng and Liu [3] conducted a stabilized mixed finite element analysis on a linear parabolic problem with Dirichlet boundary conditions. An a priori  $L^2$ -error estimate in the Crank-Nicolson fully discretized weak form was obtained. In a chosen example, suitable numerical computations were made to determine the rate of convergence of the method. In Jin et al. [4], finite element analysis on a space-fractional parabolic equation was done.

\* Corresponding author e-mail: [victor.job@uwimona.edu.jm](mailto:victor.job@uwimona.edu.jm)

The existence and uniqueness of the solution to the weak form of the problem were demonstrated. Furthermore,  $L^2$ -error estimates were produced for the semi-discrete form in the cases of smooth or non-smooth initial data. These types of estimates were also obtained for the fully discrete form, where separate cases of the Backward-Euler and the Crank-Nicolson time-stepping schemes were analyzed. Numerical computations were done to confirm the theoretical results as well. Burman et al. [5] performed a finite element analysis on the heat equation. An  $L^2$ -error estimate was obtained for the fully discretized form. Additionally, numerical computations were done to confirm the theoretical rate of convergence in space.

The finite element method is now one of the most popular tools for solving fluid-flow problems. It is widely used in solving problems involving the Stokes equation as well as the Navier-Stokes equation. These equations play huge roles in fluid dynamics, hence there are numerous recent studies on the use of the finite element method for fluid problems. Shang [6] carried out an analysis of some stabilized finite element methods for a time-dependent Stokes equation. Suitable error estimates on the semi-discrete form were obtained as well as a stability analysis of this form was performed. Appropriate numerical results were obtained to confirm the theoretical results and demonstrate that the methods suitably solve the time-dependent problem. Huang, Feng and Liu [7] applied a stabilized finite element method for the time-dependent Stokes equations using the Crank-Nicolson scheme. Suitable  $L^2$  and  $H^1$ -error estimates were obtained for the time scheme and numerical computations were performed to confirm the theoretical rates of convergence. These computations were compared with those obtained using the Backward-Euler scheme. Various plots of the Crank-Nicolson solutions were presented for different numbers of time steps and compared with that obtained when using the Backward-Euler.

Like the Stokes equations, much research has been done with regard to time-dependent Navier-Stokes equations. Jia et al. [8] analyzed the characteristic stabilized finite element method for a transient Navier-Stokes problem. The existence and uniqueness of the approximate solution were proved. Suitable theoretical error estimates on the Backward-Euler fully discretized problem were obtained. Numerical computations for the convergence rates were done for comparison to the theoretical results as well as to the previously applied Galerkin stabilized method. Li et al. [9] performed an analysis of the mixed finite element method for a time-fractional Navier-Stokes problem. Error estimates for both the semi-discrete and fully-discrete forms were produced and checked using suitable numerical computations.

A prominent field of fluid dynamics is the study of nanofluids. These fluids consist of a base fluid within which there are suspended nanoparticles. Due to the improved thermal properties over its base fluid, nanofluids are typically used as coolants in heat transfer equipment. Nanofluid models can be described as either single-phase or two-phase. One popular two-phase model is the Buongiorno model [10], which demonstrates that only Brownian diffusion and thermophoresis are important slip mechanisms in nanofluids. Particularly, the Buongiorno model has been widely investigated using different techniques such as the homotopy analysis method [11], differential transformation method [12] and finite volume method [13]. However, owing to the relative novelty of the Buongiorno model, few articles exist in the literature on two-phase nanofluid flows for which finite element analysis was conducted. Finite element analysis of a two-phase Buongiorno model was carried out by Bäsnsch [14]. The existence and uniqueness of the time-discrete weak solution were established along with bounds for this solution over time. Additionally, numerical solution plots were obtained and analyzed. Anwar [15] used the finite element method to investigate the Couette flow of a two-phase viscoelastic nanofluid. The author used a time-fractional Buongiorno model with mixed boundary conditions. Weak and semi-discrete formulations were constructed over the spatial domain, while a finite difference scheme was used to discretize in time. Using the numerical solution, the effects of important parameters were examined. Bäsnsch and Morin [16] studied the time-independent thermodynamically consistent Buongiorno model using the finite element method. The existence of regular solutions to the stationary problem was proven. Considering a family of quasi-uniform triangulations, suitable error estimates were obtained in different norms. Moreover, numerical computations were done to verify the theoretical results and to compare the effect of thermophoresis.

Based on this literature review, there is no existing study on the numerical analysis of Galerkin finite element formulations for transient two-phase Buongiorno models. In particular, error estimates for Galerkin semi-discrete and fully-discrete formulations of these unsteady nanofluid flow problems are not available in the literature. Hence, this paper seeks to analyze the Galerkin finite element method for time-dependent Poiseuille nanofluid flow using the two-phase Buongiorno model. We will derive  $L^2$ -error estimates for the velocity, temperature, and volume fraction approximations in the semi-discrete and fully-discrete cases. Using these estimates and suitable numerical computations, the rate of convergence for the finite element method will be determined.

## 2 Preliminaries

This section provides some definitions and mathematical concepts that are required for the subsequent analysis of the finite element method in this study. We use the symbol  $\Omega$  when referring to a bounded domain in  $\mathbb{R}^n$ . As usual,  $L^p(\Omega)$  denotes the space of all Lebesgue  $p$ -integrable functions on  $\Omega$ , where  $p \in \mathbb{N}$ . Also, the space  $L^\infty(\Omega)$  is the set of all essentially bounded functions on  $\Omega$ . In the present work, we denote the associated  $L^p$  norm by  $\|\cdot\|_{L^p}$  for  $1 \leq p \leq \infty$ , and the  $L^2$

inner product by  $(\cdot, \cdot)$ . The Sobolev space of order  $m \in \mathbb{N}$  in  $L^2(\Omega)$  is denoted by  $H^m(\Omega)$ , whereas  $H_0^m(\Omega)$  is defined as the subspace of  $H^m(\Omega)$  whose trace vanishes on the boundary  $\partial\Omega$ . The Sobolev norm and semi-norm are represented by  $\|\cdot\|_m$  and  $|\cdot|_m$  respectively. Where applicable, the abbreviation ‘‘a.e.’’ is used to mean ‘‘almost every’’ with respect to the Lebesgue measure.

If  $(V, \|\cdot\|_V)$  is a Banach space and  $t > 0$ , then the space  $L^2(0, \bar{t}; V)$  is defined as the set of all measurable functions  $f : (0, \bar{t}) \rightarrow V$  such that

$$\left( \int_0^{\bar{t}} \|f(s)\|_V^2 ds \right)^{1/2} < \infty.$$

The following theorem is useful for establishing the existence and uniqueness of weak solutions to parabolic problems [17, 18].

**Theorem 1. (Lions-Lax-Milgram).** *Let  $V$  and  $H$  be two Hilbert spaces,  $V \subset H$ ,  $V$  is separable and also dense in  $H$ . We identify  $H$  with its dual  $H'$  so that  $V \subset H \cong H' \subset V'$ . Let  $\bar{t} \geq 0$  and consider a mapping  $a : [0, \bar{t}] \times V \times V \rightarrow \mathbb{R}$  such that  $a(t; \cdot, \cdot)$  is bilinear for a.e.  $t \in [0, \bar{t}]$ . Moreover, assume that ‘ $a$ ’ satisfies the following properties:*

- (i) *The function  $t \rightarrow a(t; u, v)$  is measurable,  $\forall u, v \in V$ .*
- (ii)  *$\exists M$  such that  $|a(t; u, v)| \leq M \|u\|_V \|v\|_V$  for a.e.  $t \in [0, \bar{t}]$ ,  $\forall u, v \in V$ .*
- (iii)  *$\exists \alpha > 0$  and  $\gamma > 0$  such that  $a(t; u, u) + \gamma \|u\|_H^2 \geq \alpha \|u\|_V^2$  for a.e.  $t \in [0, \bar{t}]$  and  $\forall u \in V$ .*

For  $f \in L^2(0, \bar{t}; V')$  and  $u_0 \in H$ , the problem

‘‘Find  $u$  such that  $u \in L^2(0, \bar{t}; V)$ ,  $u_t \in L^2(0, \bar{t}; V')$  and

$$(u_t, v)_H + a(t; u, v) = f(t)(v), \text{ for a.e. } t \in [0, \bar{t}], \forall v \in V \tag{1}$$

with  $u(0) = u_0$ .’’  
has a unique solution.

### 3 Mathematical Model of the Problem

We consider the two-phase Poiseuille nanofluid flow between two stationary flat plates with separation  $l$ . Assuming that the fluid is Newtonian, and the flow is driven by pressure gradient  $P_x$  in the  $x$ -direction, we obtain the following parabolic system [10]:

$$\rho_{nf} u_t = -P_x + \mu_{nf} u_{zz}, \tag{2}$$

$$(\rho c)_{nf} T_t = \kappa_{nf} T_{zz} + (\rho c)_s \left[ D_B \phi_z T_z + \frac{D_T}{T_0} (T_z)^2 \right], \tag{3}$$

$$\phi_t = D_B \phi_{zz} + \frac{D_T}{T_0} T_{zz}, \tag{4}$$

for  $(z, t) \in (0, l) \times (0, \infty)$ , with initial conditions

$$u = 0, T = T_0, \phi = \phi_0 \text{ for } (z, t) \in [0, l] \times \{0\} \tag{5}$$

and boundary conditions

$$u = 0, T = T_0, \phi = \phi_0 \text{ for } (z, t) \in \{0\} \times (0, \infty), \tag{6}$$

$$u = 0, T = T_1, \phi = \phi_0 \text{ for } (z, t) \in \{l\} \times (0, \infty). \tag{7}$$

In the aforementioned equations, the symbols  $u, T, \phi$  are the flow velocity, nanofluid temperature and volume fraction of the nanoparticle, respectively. The constants  $\rho_{nf}, c_{nf}, \kappa_{nf}, \mu_{nf}$  represents the density, heat capacity, thermal conductivity, and viscosity of the nanofluid while  $\rho_s, c_s, D_T, D_B$  represent the nanoparticle density, specific heat, thermophoretic diffusivity and Brownian diffusivity, respectively. Equations (2) to (4) and the initial and boundary conditions (5) to (7) can be written in vector form as

$$A_0 X_t = B_0 X_{zz} + F(t, X), \tag{8}$$

$$X(z, 0) = \begin{bmatrix} 0 \\ T_0 \\ \phi_0 \end{bmatrix} = X_0, \forall z \in [0, l], \tag{9}$$

$$X(0,t) = \begin{bmatrix} 0 \\ T_0 \\ \phi_0 \end{bmatrix}, X(l,t) = \begin{bmatrix} 0 \\ T_1 \\ \phi_0 \end{bmatrix}, \forall t > 0, \quad (10)$$

where

$$X = \begin{bmatrix} u \\ T \\ \phi \end{bmatrix}, A_0 = \begin{bmatrix} \rho_{nf} & 0 & 0 \\ 0 & (\rho c)_{nf} & 0 \\ 0 & 0 & 1 \end{bmatrix}, B_0 = \begin{bmatrix} \mu_{nf} & 0 & 0 \\ 0 & \kappa_{nf} & 0 \\ 0 & 0 & D_B \end{bmatrix}$$

and

$$F(t,X) = \begin{bmatrix} -P_x \\ (\rho c)_s [D_B \phi_z T_z + \frac{D_T}{T_0} (T_z)^2] \\ \frac{D_T}{T_0} T_{zz} \end{bmatrix} = \begin{bmatrix} -P_x \\ f(X) \\ \frac{D_T}{T_0} T_{zz} \end{bmatrix}.$$

## 4 Galerkin Finite Element Method

In this section, we analyze the Galerkin finite element formulation of (8)-(10) under the following fixed-point iteration

$$A_0 X_t^{k+1} = B_0 X_{zz}^{k+1} + F(t, X^k), \quad (11)$$

$$X^{k+1}(z, 0) = \begin{bmatrix} 0 \\ T_0 \\ \phi_0 \end{bmatrix} = X_0, \forall z \in [0, l], \quad (12)$$

$$X^{k+1}(0, t) = \begin{bmatrix} 0 \\ T_0 \\ \phi_0 \end{bmatrix}, X^{k+1}(l, t) = \begin{bmatrix} 0 \\ T_1 \\ \phi_0 \end{bmatrix}, \forall t > 0, \quad (13)$$

where  $k = 0, 1, 2, \dots$

### 4.1 Weak Formulation

Let  $V = (H_0^1(0, l))^3$ . Suppose that  $\tilde{T}, \tilde{\phi} \in H^1(0, l)$  such that

$$\tilde{T}(0) = T_0, \tilde{T}(l) = T_1, \tilde{\phi}(0) = \phi_0 = \tilde{\phi}(l),$$

and define  $\tilde{X} = \begin{bmatrix} 0 \\ \tilde{T} \\ \tilde{\phi} \end{bmatrix}$ . Then, the weak formulation can be written as:

Given  $t \geq 0$  and  $X^k \in L^2(0, \bar{t}; (H^1(0, l))^3)$  for  $k = 0, 1, 2, \dots$ , find  $X^{k+1}$  such that  $X^{k+1} - X \in L^2(0, \bar{t}; V)$ ,  $X_t^{k+1} \in L^2(0, \bar{t}; V')$  and

$$(X_t^{k+1}, W)_{(L^2)^3} + (A_0^{-1} B_0 X_z^{k+1}, W_z)_{(L^2)^3} = g(t, X^k, W), \forall W \in V, \quad (14)$$

with  $X^{k+1}(0) = X_0$ . In equation (14), the symbol  $(\cdot, \cdot)_{(L^2)^3}$  represents the  $(L^2(0, l))^3$  inner product,

$$g(t, X^k, W) = (A_0^{-1} [-P_x, f(X^k), 0]', W)_{(L^2)^3} + \left( [0, 0, -\frac{D_T}{T_0} T_z^k]', W_z \right)_{(L^2)^3},$$

and the notation  $[\cdot]'$  refers to the matrix transpose operator.

**Theorem 2.** *The weak formulation has a unique solution provided that  $P_x \in L^2(0, \bar{t})$ .*

*Proof.*(i) Existence: If  $X_*^{k+1}(t) = X^{k+1}(t) - \tilde{X}$ , then we have  $X^{k+1}(t) = X_*^{k+1}(t) + \tilde{X}$ . For  $p, q \in V$ , let  $a(t; p, q) = (A_0^{-1}B_0p_z, q_z)_{(L^2)^3}$ . Then (14) becomes

$$(X_*^{k+1}, W)_{(L^2)^3} + a(t; X_*^{k+1}, W) = G_k(t)(W), \tag{15}$$

where  $G_k(t)(W) = g(t, X^k, W) - (A_0^{-1}B_0\tilde{X}, W_z)_{(L^2)^3}$ .

It is clear that the function  $t \rightarrow a(t; p, q)$  is measurable  $\forall p, q \in V$ .

Choose  $a_0 = \max \left\{ \frac{\mu_{nf}}{\rho_{nf}}, \frac{\kappa_{nf}}{(\rho c)_{nf}}, D_B \right\}$  and  $\bar{a}_0 = \min \left\{ \frac{\mu_{nf}}{\rho_{nf}}, \frac{\kappa_{nf}}{(\rho c)_{nf}}, D_B \right\}$ .

Using the Cauchy-Schwarz inequality, we get

$$|a(t; p, q)| = \left| (A_0^{-1}B_0p_z, q_z)_{(L^2)^3} \right| \leq \|A_0^{-1}B_0p_z\|_{(L^2)^3} \|q_z\|_{(L^2)^3} \leq a_0 \|p_z\|_{(L^2)^3} \|q_z\|_{(L^2)^3} = a_0 \|p\|_V \|q\|_V,$$

where  $\|\cdot\|_V$  represents the natural norm on  $V$ . Thus, for a fixed  $t$ , the bilinear form  $a(t; \cdot, \cdot)$  is continuous on  $V$ . Furthermore,

$$a(t; p, p) + \|p\|_{(L^2)^3}^2 \geq a(t; p, p) = (A_0^{-1}B_0p_z, p_z)_{(L^2)^3} \geq \bar{a}_0 (p_z, p_z)_{(L^2)^3} = \bar{a}_0 \|p\|_V^2.$$

Now, let  $B_1^k(t) = [-P_x, f(X^k), 0]'$  and  $B_2^k(t) = [0, 0, -D_T/T_0T_z^k]'$ . By the Poincaré inequality there exists  $C > 0$  such that

$$|G_k(t)(W)| \leq \left[ C \|A_0^{-1}B_1^k(t)\|_{(L^2)^3} + \|B_2^k(t)\|_{(L^2)^3} + \|A_0^{-1}B_0\tilde{X}\|_{(L^2)^3} \right] \|W\|_V = \bar{C}(t) \|W\|_V.$$

Thus, for each  $t \in [0, \bar{t}]$ ,  $G_k(t) \in V'$ .

Since  $\frac{\partial P}{\partial x}(\cdot), \|f_2(X^k)\|_{L^2}(\cdot), \|T_z^k\|_{L^2}(\cdot) \in L^2(0, \bar{t})$  then

$$\|A_0^{-1}B_1^k\|_{(L^2)^3}(\cdot), \|A_0^{-1}B_0\tilde{X}\|_{(L^2)^3}(\cdot), \|B_2^k\|_{(L^2)^3}(\cdot) \in L^2(0, \bar{t}).$$

Hence, we have

$$\int_0^{\bar{t}} \|G_k(t)\|_{V'}^2 dt \leq \int_0^{\bar{t}} \bar{C}(t)^2 dt < \infty,$$

which implies that  $G_k \in L^2(0, \bar{t}; V')$ .

Thus, by Theorem 1, a unique solution  $X_*^{k+1}$  exists for (15). This implies that there exists such a solution  $X^{k+1}$  to our original weak formulation.

(ii) Uniqueness: Suppose that  $X_1^{k+1}$  is another solution to our weak formulation. Then we have

$$(X_t^{k+1} - X_{1,t}^{k+1}, W)_{(L^2)^3} + a(t; X^{k+1} - X_1^{k+1}, W) = 0, \forall W \in V.$$

Since  $X^{k+1} - X_1^{k+1} \in V$ , then by Gronwall's lemma,

$$0 \leq \|X^{k+1} - X_1^{k+1}\|_{(L^2)^3}^2 \leq \|X^{k+1}(0) - X_1^{k+1}(0)\|_{(L^2)^3}^2 = 0.$$

This implies  $X^{k+1} = X_1^{k+1}$ .

### 4.2 Galerkin Semi-Discrete Formulation

In this section, we construct the spatial Galerkin formulation of the problem. The existence and uniqueness of the solution to the semi-discrete formulation are discussed. Furthermore,  $L^2$ -error estimates for this solution are obtained.

Let  $\tau^h$  be a triangulation of the interval  $(0, l)$  with mesh parameter

$$h = \max_{E \in \tau^h} \text{diam}(E).$$

We consider the finite-dimensional piecewise  $m^{\text{th}}$ -degree polynomial space

$$\widehat{S}_h = \left\{ q_h \in C[0, l] : q_h|_E \in \mathbb{P}_m(E), \forall E \in \tau^h \right\} \cap H_0^1(0, l)$$

and the associated product space  $S_h = (\widehat{S}_h)^3$ . We state our semi-discrete formulation as:

Given  $\bar{t} > 0, k = 0, 1, 2, \dots$  and  $X_h^k \in L^2\left(0, \bar{t}; (H^1(0, l))^3\right)$ , find  $X_h^{k+1}$  such that  $X_h^{k+1} - \tilde{X} \in L^2(0, \bar{t}; S_h), X_{h,t}^{k+1} \in L^2\left(0, \bar{t}; S'_h\right)$

and

$$(X_{h,t}^{k+1}, W_h)_{(L^2)^3} + (A_0^{-1} B_0 X_{h,z}^{k+1}, W_{h,z})_{(L^2)^3} = g(t, X_h^k, W_h), \quad \forall W_h \in S_h, \quad (16)$$

$$\text{with } X_h^{k+1}(0) = \begin{bmatrix} 0 \\ T_0 \\ \phi_0 \end{bmatrix}.$$

The existence and uniqueness of the solution to (16) follows from the well-known theory and analysis of ordinary differential equations (see Braun [19]).

We now derive  $L^2$ -error estimates between the weak solution  $X^{k+1} = [u, T^{k+1}, \phi^{k+1}]'$  and the corresponding semi-discrete solution  $X_h^{k+1} = [u_h, T_h^{k+1}, \phi_h^{k+1}]'$ . For these estimates, we have the following interpolation property [20]:

$$\|v - \mathcal{I}_h v\|_{L^2} \leq Ch^{m+1} \|v\|_{m+1}, \quad \forall v \in H^{m+1}(0, l) \cap H_0^1(0, l), \quad (17)$$

where  $\mathcal{I}_h : H^{m+1}(0, l) \cap H_0^1(0, l) \rightarrow \widehat{S}_h$  is an interpolation operator.

**Theorem 3.** For  $k = 0, 1, 2, \dots$ , let  $X^{k+1}$  and  $X_h^{k+1}$  be the solutions to (14) and (16) respectively. Suppose that

$$u(t), T^{k+1}(t) - \tilde{T}, \phi^{k+1}(t) - \tilde{\phi} \in H^{m+1}(0, l)$$

for  $t \in (0, \bar{t}]$ ,

$$u_t, T_t^{k+1}, \phi_t^{k+1} \in L^2(0, \bar{t}; H^{m+1}(0, l)),$$

and  $J^k = D_B \phi_z^k + \frac{D_T}{T_0} T_z^k \in L^2(0, \bar{t}; L^\infty(0, l))$ . Then for some  $C > 0$ , the following hold:

$$\|u_h(t) - u(t)\|_{L^2} \leq 2Ch^{m+1} \int_0^t \|u_t(s)\|_{m+1} ds, \quad (18)$$

$$\begin{aligned} \|T_h^{k+1}(t) - T^{k+1}(t)\|_{L^2} &\leq 2Ch^{m+1} \left[ \|T_0 - \tilde{T}\|_{m+1} + \int_0^t \|T_t^{k+1}(s)\|_{L^2} ds \right] + \frac{(\rho c)_s}{(\rho c)_{nf}} \int_0^t \|J_h^k(s) - J^k(s)\|_{L^\infty} \|T_z^k(s)\|_{L^2} ds \\ &+ \frac{(\rho c)_s}{(\rho c)_{nf}} \int_0^t \left( \|J_h^k(s) - J^k(s)\|_{L^\infty} + \|J^k(s)\|_{L^\infty} \right) \|T_{h,z}^k(s) - T_z^k(s)\|_{L^2} ds \end{aligned} \quad (19)$$

and

$$\|\phi_h^{k+1}(t) - \phi^{k+1}(t)\|_{L^2} \leq 2Ch^{m+1} \left[ \|\phi_0 - \tilde{\phi}\|_{m+1} + \int_0^t \|\phi_t^{k+1}(s)\| ds \right] + \frac{D_T}{T_0} \|D_z\|_{\widehat{S}_h, L^2} \int_0^t \|T_{h,z}^k(s) - T_z^k(s)\| ds. \quad (20)$$

*Proof:* To obtain (18), let  $\theta_u(t) = u_h(t) - R_h u(t)$  and  $\chi_u(t) = R_h u(t) - u(t)$ , where  $R_h : H_0^1(0, l) \rightarrow \widehat{S}_h$  is the Ritz projection onto  $\widehat{S}_h$ . Then we can write  $u_h(t) - u(t) = \theta_u(t) + \chi_u(t)$ . By the interpolation property (17), we have

$$\|\chi_u(t)\|_{L^2} = \|u_h(t) - R_h u(t)\|_{L^2} \leq Ch^{m+1} \|u(t)\|_{m+1} \leq Ch^{m+1} \int_0^t \|u_t(s)\|_{m+1} ds.$$

Also, from the first components of the vector equations (14) and (16),

$$\rho_{nf}(\theta_{u,t}, w_{1h}) + \mu_{nf}(\theta_{u,z}, w_{1h,z}) = -\rho_{nf}(R_h u_t - u_t, w_{1h}) = -\rho_{nf}(\chi_{u,t}, w_{1h}), \quad \forall w_{1h} \in \widehat{S}_h.$$

Since  $\theta_u \in \widehat{S}_h$ , we can choose  $w_{1h} = \theta_u$  to obtain

$$\rho_{nf}(\theta_{u,t}, \theta_u) + \mu_{nf} \|\theta_{u,z}\|_{L^2}^2 = -\rho_{nf}(\chi_t, \theta_u) \Rightarrow \|\theta_u(t)\|_{L^2} \frac{d}{dt} \|\theta_u(t)\|_{L^2} \leq \|\chi_{u,t}(t)\|_{L^2} \|\theta_u(t)\|_{L^2}.$$

If  $\|\theta_u(t)\|_{L^2} = 0$ , then our desired result would be trivially true. Hence, by assuming that  $\|\theta_u(t)\|_{L^2} \neq 0$  and applying Grönwall's inequality, we get

$$\|\theta_u(t)\|_{L^2} \leq \|\theta_u(0)\|_{L^2} + \int_0^t \|\chi_{u,t}(s)\|_{L^2} ds.$$

Since  $\|\chi_{u,t}(t)\|_{L^2} = \|\mathcal{R}_h u_t(t) - u_t(t)\|_{L^2} \leq Ch^{m+1} \|u_t(t)\|_{m+1}$  and

$$\|\theta_u(0)\|_{L^2} = \|u_h(0) - \mathcal{R}_h u(0)\|_{L^2} \leq Ch^{m+1} \|u(0)\|_{m+1} = 0,$$

then we arrive at the desired inequality

$$\|u_h(t) - u(t)\|_{L^2} \leq 2Ch^{m+1} \int_0^t \|u_t(s)\|_{m+1} ds.$$

To obtain (19), let  $T_*^{k+1}(t) = T^{k+1}(t) - \tilde{T}$ ,  $T_{*h}^{k+1}(t) = T_h^{k+1}(t) - \tilde{T}$ , and take  $\theta_T^{k+1}(t) = T_*^{k+1}(t) - \mathcal{R}_h T_*^{k+1}(t)$  and  $\chi_T^{k+1}(t) = \mathcal{R}_h T_*^{k+1}(t) - T_*^{k+1}(t)$ . Similar to the case of the velocity, we have

$$\|\chi_T^{k+1}(t)\|_{L^2} \leq Ch^{m+1} \left( \|T_0 - \tilde{T}\|_{m+1} + \int_0^t \|T_t^{k+1}(s)\|_{m+1} ds \right).$$

Also, for every  $w_{2h} \in \widehat{S}_h$ ,

$$(\rho c)_{nf}(\theta_{T,t}^{k+1}, w_{2h}) + \kappa_{nf}(\theta_{T,z}^{k+1}, w_{2h,z}) = (f(X_h^k) - f(X^k), w_{2h}) - (\rho c)_{nf}(\chi_{T,t}^{k+1}, w_{2h}).$$

Taking  $w_{2h} = \theta_T^{k+1}$  gives

$$\|\theta_T^{k+1}(t)\|_{L^2} \leq \|\theta_T^{k+1}(0)\|_{L^2} + \int_0^t \|\chi_{T,t}^{k+1}(s)\|_{L^2} ds + \frac{1}{(\rho c)_{nf}} \int_0^t \|f(X_h^k) - f(X^k)\|_{L^2} ds.$$

Now, if we define  $J_h^k = D_B \phi_{h,z}^k - \frac{D_T}{T_0} T_{h,z}^k$ , then

$$\|f(X_h^k) - f(X^k)\|_{L^2} = (\rho c)_s \|T_{h,z}^k J_h^k - T_z^k J^k\|_{L^2} \leq (\rho c)_s (\|J_h^k - J^k\|_{L^\infty} + \|J^k\|_{L^\infty}) \|T_{h,z}^k - T_z^k\|_{L^2} + (\rho c)_s \|J_h^k - J^k\|_{L^\infty} \|T_z^k\|_{L^2}.$$

Thus, with  $\|\theta_T^{k+1}(0)\|_{L^2} \leq Ch^{m+1} \|T_0 - \tilde{T}\|_{m+1}$  and  $\|\chi_{T,t}^{k+1}\|_{L^2} \leq Ch^{m+1} \|T_t^{k+1}(t)\|_{m+1}$ , we get

$$\begin{aligned} \|T_h^{k+1}(t) - T^{k+1}(t)\|_{L^2} &\leq 2Ch^{m+1} \left( \|T_0 - \tilde{T}\|_{m+1} + \int_0^t \|T_t(s)\|_{m+1} ds \right) + \frac{(\rho c)_s}{(\rho c)_{nf}} \int_0^t \|J_h^k(s) - J^k(s)\|_{L^\infty} \|T_z^k(s)\|_{L^2} ds \\ &\quad + \frac{(\rho c)_s}{(\rho c)_{nf}} \int_0^t (\|J_h^k(s) - J^k(s)\|_{L^\infty} + \|J^k(s)\|_{L^\infty}) \|T_{h,z}^k(s) - T_z^k(s)\|_{L^2} ds. \end{aligned}$$

For the final estimate (20), let  $\phi_*^{k+1}(t) = \phi^{k+1}(t) - \tilde{\phi}$  and  $\phi_{*h}^{k+1}(t) = \phi_h^{k+1}(t) - \tilde{\phi}$  and take  $\theta_\phi^{k+1}(t) = \phi_*^{k+1}(t) - \mathcal{R}_h \phi_*^{k+1}(t)$  and  $\chi_\phi^{k+1}(t) = \mathcal{R}_h \phi_*^{k+1}(t) - \phi_*^{k+1}(t)$ . In a similar manner to the temperature estimate, we have

$$\|\chi_\phi^{k+1}(t)\|_{L^2} \leq Ch^{m+1} \left( \|\phi_0 - \tilde{\phi}\|_{m+1} + \int_0^t \|\phi_t^{k+1}(s)\|_{m+1} ds \right)$$

and

$$\|\theta_\phi^{k+1}(t)\|_{L^2} \leq Ch^{m+1} \left( \|\phi_0 - \tilde{\phi}\|_{m+1} + \int_0^t \|\phi_t^{k+1}(s)\|_{m+1} ds \right) + \frac{D_T}{T_0} \|D_z\|_{\widehat{S}_h, L^2} \int_0^t \|T_{h,z}^k(s) - T_z^k(s)\|_{L^2} ds,$$

where  $\|D_z\|_{\widehat{S}_h, L^2}$  represents the operator norm of the weak derivative operator  $D_z: \widehat{S}_h \rightarrow L^2(0, l)$  defined by

$$D_z v = v_z, \forall v \in \widehat{S}_h.$$

Hence by the triangle inequality, we have the estimate

$$\|\phi_h^{k+1}(t) - \phi^{k+1}(t)\|_{L^2} \leq 2Ch^{m+1} \left[ \|\phi_0 - \tilde{\phi}\|_{m+1} + \int_0^t \|\phi_t^{k+1}(s)\|_{m+1} ds \right] + \frac{D_T}{T_0} \|D_z\|_{\widehat{S}_h, L^2} \int_0^t \|T_{h,z}^k(s) - T_z^k(s)\|_{L^2} ds.$$

**Corollary 1.** Let the assumptions of Theorem 3 hold and suppose that there exist positive constants  $D_1^k, D_2^k$  and  $D_3$  such that for a.e.  $t \in [0, \bar{t}]$ ,

$$\|T_{h,z}^k(t) - T_z^k(t)\|_{L^2} \leq D_1^k h^{m+1}, \|J_h^k(t) - J^k(t)\|_{L^\infty} \leq D_2^k h^{m+1} \text{ and } \|D_z\|_{\widehat{S}_h, L^2} \leq D_3.$$

Then  $\|X_h^{k+1}(t) - X^{k+1}(t)\|_{(L^2)^3} \in O(h^{m+1})$  as  $h \rightarrow 0$  and

$$\lim_{h \rightarrow 0} \|X_h^{k+1}(t) - X^{k+1}(t)\|_{(L^2)^3} = 0.$$

*Proof.* This follows directly from the inequalities (18) to (20) in Theorem 3.

### 5 Fully-Discrete Formulation

In this section, we perform a time discretization of the problem by applying the backward-Euler scheme to the semi-discrete equation (16). Let  $t_1, t_2, \dots, t_N$  be equally spaced points in  $[0, \bar{t}]$  such that

$$t_1 = 0 < t_2 < t_3 < \dots < t_N = \bar{t}.$$

Define  $\Delta t = t_n - t_{n-1}, \forall n = 2, 3, \dots, N$  and consider the backward-difference operator

$$D^- X_h^{k+1, n} = \frac{X_h^{k+1, n} - X_h^{k+1, n-1}}{\Delta t},$$

where

$$X_h^{k+1}(t_n) = \begin{bmatrix} u_h(t_n) \\ T_h^{k+1}(t_n) \\ \phi_h^{k+1}(t_n) \end{bmatrix} \simeq \begin{bmatrix} u_h^n \\ T_h^{k+1, n} \\ \phi_h^{k+1, n} \end{bmatrix} = X_h^{k+1, n}.$$

For  $X_h^{k+1, n} - \tilde{X} \in S_h$ , we obtain the fully discrete form

$$(D^- X_h^{k+1, n}, W_h)_{(L^2)^3} + (A_0^{-1} B_0 X_{h,z}^{k+1, n}, W_{h,z})_{(L^2)^3} = g(t_n, X_h^{k, n}, W_h), \forall W_h \in S_h. \tag{21}$$

In the following theorem,  $L^2$  error estimates are obtained for the fully discrete Galerkin finite element solution of equation (21).

**Theorem 4.** For  $k = 0, 1, 2, \dots$ , and  $n = 2, 3, \dots, N$ , let  $X^{k+1}(t_n)$  and  $X_h^{k+1, n}$  be the solutions to (14) and (21) respectively. Suppose that  $u(t_n), T^{k+1}(t_n) - \tilde{T}, \phi^{k+1}(t_n) - \tilde{\phi} \in H^{m+1}(0, l); u_t, T_t^{k+1}, \phi_t^{k+1} \in L^2(0, \bar{t}; H^{m+1}(0, l));$  and  $u_n, T_n^{k+1}, \phi_n^{k+1} \in L^2(0, \bar{t}; L^2(0, l))$ . Then

$$\begin{aligned} \|u_h^n - u(t_n)\|_{L^2} &\leq 2Ch^{m+1} \int_0^{t_n} \|u_t(s)\|_{m+1} ds + \Delta t \int_0^{t_n} \|u_{tt}(s)\|_{L^2} ds, \\ \|T_h^{k+1, n} - T^{k+1}(t_n)\|_{L^2} &\leq 2Ch^{m+1} \left[ \|T_0 - \tilde{T}\|_{m+1} + \int_0^{t_n} \|T_t^{k+1}(s)\|_{m+1} ds \right] \\ &\quad + \frac{\Delta t (\rho c)_s}{(\rho c)_{nf}} \sum_{j=2}^n \left( \|J_h^{k, j} - J^k(t_j)\|_{L^\infty} + \|J^k(t_j)\|_{L^\infty} \right) \|T_{h,z}^{k, j} - T_z^k(t_j)\|_{L^2} \end{aligned} \tag{22}$$

$$+ \frac{\Delta t (\rho c)_s}{(\rho c)_{nf}} \sum_{j=2}^n \|J_h^{k,j} - J^k(t_j)\|_{L^\infty} \|T_z^k(t_j)\|_{L^2} + \Delta t \int_0^{t_n} \|T_{tt}^{k+1}(s)\|_{L^2} ds \tag{23}$$

and

$$\begin{aligned} \|\phi_h^{k+1,n} - \phi^{k+1}(t_n)\|_{L^2} &\leq 2Ch^{m+1} \left[ \|\phi_0 - \tilde{\phi}\|_{m+1} + \int_0^{t_n} \|\phi_t^{k+1}(s)\|_{m+1} ds \right] \\ &+ \Delta t \int_0^{t_n} \|\phi_{tt}^{k+1}(s)\|_{L^2} ds + \frac{DT\Delta t}{T_0} \|D_z\|_{\widehat{S}_h, L^2} \sum_{j=2}^n \|T_{h,z}^{k,j} - T_z^k(t_j)\|_{L^2}. \end{aligned} \tag{24}$$

*Proof.* We first obtain the velocity estimate (22) by taking  $u_h^n - u(t_n) = \theta_u^n + \chi_u^n$ , where  $\theta_u^n = u_h^n - R_h u(t_n)$  and  $\chi_u^n = R_h u(t_n) - u(t_n)$ . Using a similar approach to the semi-discrete estimate (18), we have

$$\|\chi_u^n\|_{L^2} \leq Ch^{m+1} \int_0^{t_n} \|u_t(s)\|_{m+1} ds.$$

Now for every  $w_{1h} \in \widehat{S}_h$ ,

$$\rho_{nf}(D^- \theta_u^n, w_{1h}) + \mu_{nf}(\theta_{u,z}^n, w_{1h,z}) = -\rho_{nf}(\lambda_u^n, w_{1h}),$$

where

$$\lambda_u^n = R_h D^- u(t_n) - u_t(t_n) = [R_h D^- u(t_n) - D^- u(t_n)] + [D^- u(t_n) - u_t(t_n)] = \lambda_{1u}^n + \lambda_{2u}^n.$$

Taking  $w_{1h} = \theta_u^n$ ,

$$\rho_{nf}(D^- \theta_u^n, \theta_u^n) + \mu_{nf} \|\theta_{u,z}^n\|_{L^2}^2 = -\rho_{nf}(\lambda_u^n, \theta_u^n)$$

implies that

$$\|\theta_u^n\|_{L^2} \leq \|\theta_u^{n-1}\|_{L^2} + \Delta t \|\lambda_u^n\|_{L^2}.$$

By repeated application of the aforementioned inequality, we have

$$\|\theta_u^n\|_{L^2} \leq \|\theta_u^1\|_{L^2} + \Delta t \sum_{j=2}^n \|\lambda_u^j\|_{L^2} \leq \Delta t \sum_{j=2}^n \|\lambda_{1u}^j\|_{L^2} + \Delta t \sum_{j=2}^n \|\lambda_{2u}^j\|_{L^2}.$$

We note that for each  $j = 2, 3, \dots, n$ ,

$$\lambda_{1u}^j = (R_h - I)D^- u(t_j) = (R_h - I) \frac{1}{\Delta t} \int_{t_{j-1}}^{t_j} u_t(s) ds,$$

where  $I$  is the identity operator on  $H_0^1(0, l)$ . Hence,

$$\|\lambda_{1u}^j\|_{L^2} \leq \frac{1}{\Delta t} Ch^{m+1} \int_{t_{j-1}}^{t_j} \|u_t(s)\|_{m+1} ds \Rightarrow \Delta t \sum_{j=2}^n \|\lambda_{1u}^j\|_{L^2} \leq Ch^{m+1} \int_0^{t_n} \|u_t(s)\|_{m+1} ds.$$

Also, since

$$\Delta t \lambda_{2u}^j = \Delta t D^- u(t_j) - \Delta t u_t(t_j) = - \int_{t_{j-1}}^{t_j} (s - t_{j-1}) u_{tt}(s) ds,$$

we obtain

$$\Delta t \sum_{j=2}^n \|\lambda_{2u}^j\|_{L^2} \leq \Delta t \int_0^{t_n} \|u_{tt}(s)\|_{L^2} ds.$$

This leads to the inequality

$$\|\theta_u^n\|_{L^2} \leq Ch^{m+1} \int_0^{t_n} \|u_t(s)\|_{m+1} ds + \Delta t \int_0^{t_n} \|u_{tt}(s)\|_{L^2} ds.$$

Hence the desired velocity estimate is

$$\|u_h^n - u(t_n)\|_{L^2} \leq 2Ch^{m+1} \int_0^{t_n} \|u_t(s)\|_{m+1} ds + \Delta t \int_0^{t_n} \|u_{tt}(s)\|_{L^2} ds.$$

Now for the temperature estimate (23), let  $T_*^{k+1,n} = T_h^{k+1,n} - \tilde{T}$ ,  $T_*^{k+1}(t_n) = T^{k+1}(t_n) - \tilde{T}$ , and take  $\theta_T^{k+1,n} = T_*^{k+1,n} - R_h T_*^{k+1}(t_n)$  and  $\chi_T^{k+1,n} = R_h T_*^{k+1}(t_n) - T_*^{k+1}(t_n)$ . Then we can see that

$$\|\chi_T^{k+1,n}\|_{L^2} \leq Ch^{m+1} \left[ \|T_0 - \tilde{T}\|_{m+1} + \int_0^{t_n} \|T_t^{k+1}(s)\|_{m+1} ds \right]$$

and

$$\begin{aligned} \|\theta_T^{k+1,n}\|_{L^2} &\leq Ch^{m+1} \left[ \|T_0 - \tilde{T}\|_{m+1} + \int_0^{t_n} \|T_t^{k+1}(s)\|_{m+1} ds \right] + Ch^{m+1} \int_0^{t_n} \|T_t^{k+1}(s)\|_{m+1} ds \\ &+ \Delta t \int_0^{t_n} \|T_{tt}^{k+1}(s)\|_{L^2} ds + \frac{\Delta t}{(\rho c)_{nf}} \sum_{j=2}^n \|f(X_h^{k,n}) - f(X^k(t_n))\|_{L^2}. \end{aligned}$$

Since

$$\begin{aligned} \frac{\Delta t}{(\rho c)_{nf}} \sum_{j=2}^n \|f(X_h^{k,n}) - f(X^k(t_n))\|_{L^2} &\leq \frac{\Delta t (\rho c)_s}{(\rho c)_{nf}} \sum_{j=2}^n \left( \|J_h^{k,j} - J^k(t_j)\|_{L^\infty} + \|J^k(t_j)\|_{L^\infty} \right) \|T_{h,z}^{k,j} - T_z^k(t_j)\|_{L^2} \\ &+ \frac{\Delta t (\rho c)_s}{(\rho c)_{nf}} \sum_{j=2}^n \|J_h^{k,j} - J^k(t_j)\|_{L^\infty} \|T_z^k(t_j)\|_{L^2}, \end{aligned}$$

then the temperature estimate (23) is obtained as

$$\begin{aligned} \|T_h^{k+1,n} - T^{k+1}(t_n)\|_{L^2} &\leq 2Ch^{m+1} \left[ \|T_0 - \tilde{T}\|_{m+1} + \int_0^{t_n} \|T_t^{k+1}(s)\|_{m+1} ds \right] + \Delta t \int_0^{t_n} \|T_{tt}^{k+1}(s)\|_{L^2} ds \\ &+ \frac{\Delta t (\rho c)_s}{(\rho c)_{nf}} \sum_{j=2}^n \left( \|J_h^{k,j} - J^k(t_j)\|_{L^\infty} + \|J^k(t_j)\|_{L^\infty} \right) \|T_{h,z}^{k,j} - T_z^k(t_j)\|_{L^2} + \frac{\Delta t (\rho c)_s}{(\rho c)_{nf}} \sum_{j=2}^n \|J_h^{k,j} - J^k(t_j)\|_{L^\infty} \|T_z^k(t_j)\|_{L^2}. \end{aligned}$$

Finally, to obtain the volume fraction estimate (24) we define  $\phi_*^{k+1,n} = \phi_h^{k+1,n} - \tilde{\phi}$ ,  $\phi_*^{k+1,n} = \phi^{k+1,n} - \tilde{\phi}$ ,  $\theta_\phi^{k+1,n} = \phi_*^{k+1,n} - R_h \phi_*^{k+1}(t_n)$  and  $\chi_\phi^{k+1,n} = R_h \phi_*^{k+1}(t_n) - \phi_*^{k+1}(t_n)$ . Then

$$\|\chi_\phi^{k+1,n}\|_{L^2} \leq Ch^{m+1} \left[ \|\phi_0 - \tilde{\phi}\|_{m+1} + \int_0^{t_n} \|\phi_t^{k+1}(s)\|_{m+1} ds \right]$$

and

$$\begin{aligned} \|\theta_\phi^{k+1,n}\|_{L^2} &\leq Ch^{m+1} \left[ \|\phi_0 - \tilde{\phi}\|_{m+1} + \int_0^{t_n} \|\phi_t^{k+1}(s)\|_{m+1} ds \right] + \Delta t \int_0^{t_n} \|\phi_{tt}^{k+1}(s)\| ds \\ &+ \frac{D_T \Delta t}{T_0} \|D_z\|_{\hat{S}_h, L^2} \sum_{j=2}^n \|T_{h,z}^{k,j} - T_z^k(t_j)\|_{L^2}. \end{aligned}$$

The volume fraction estimate (24) follows from the triangle inequality.

**Corollary 2.** Let the assumptions of Theorem 4 hold and suppose for each  $j = 2, 3, \dots, N$ , there exists positive real numbers  $D_1^{k,j}$ ,  $D_2^{k,j}$  and  $D_3$  such that

$$\|T_{h,z}^{k,j} - T_z^k(t_j)\|_{L^2} \leq D_1^{k,j} h^{m+1}, \quad \|J_h^{k,j} - J^k(t_j)\|_{L^\infty} \leq D_2^{k,j} h^{m+1} \quad \text{and} \quad \|D_z\|_{\hat{S}_h, L^2} \leq D_3.$$

Then  $\|X_h^{k+1,n} - X^{k+1}(t_n)\|_{(L^2)^3} \in O(h^{m+1}) + O(\Delta t)$  and

$$\lim_{(h, \Delta t) \rightarrow 0} \|X_h^{k+1,n} - X^{k+1}(t_n)\|_{(L^2)^3} = 0.$$

*Proof.* This is a direct consequence of the fully-discrete error estimates (22) to (24).

## 6 Numerical Computations and Results

In this section, a numerical example is considered for the implementation of the finite element method as analyzed in Sections 4 and 5. For this example, we consider the Poiseuille flow of an alumina-water nanofluid, with plate separation  $l = 1\text{m}$ . We will assume that the water is pure and that the alumina nanoparticles are spherical with diameter  $10\text{nm}$ . The temperature on the lower and upper plates are taken to be  $298.15\text{K}$ ,  $308.15\text{K}$ , respectively. We take the nanoparticle volume fraction to be  $0.05$ , and assume that the flow be driven by oscillating pressure gradient

$$P_x(t) = - \left( 0.1 + 0.5 \sin \frac{10\pi t}{\bar{t}} \right).$$

The density  $\rho_{bf}$ , specific heat  $c_{bf}$ , thermal conductivity  $\kappa_{bf}$  and viscosity  $\mu_{bf}$  of pure water at  $298.15\text{K}$  are  $997.1\text{kg/m}^3$ ,  $4183\text{J}/(\text{kg}\cdot\text{K})$ ,  $0.5948\text{W}/(\text{m}\cdot\text{K})$  and  $8.905 \times 10^{-4}\text{Pa}\cdot\text{s}$  [21]. The specific heat and density of the nanoparticles are  $775\text{J}/(\text{kg}\cdot\text{K})$  and  $388\text{kg/m}^3$ , respectively [22]. Using these values,  $\rho_{nf}$ ,  $c_{nf}$ ,  $\mu_{nf}$ ,  $\kappa_{nf}$ ,  $D_B$  and  $D_T$  can be calculated from their respective formulae in Bounghorno [10].

Following the fully-discrete formulation in Section 5, suppose that the triangulation  $\tau^h$  consists of  $N_{el}$  quadratic line elements ( $m = 2$ ). Let  $\{\psi_j\}_{j=1}^{N_h}$  be the Lagrange basis for the piecewise quadratic function space

$$P_h = \{q_h \in C[0, l] : q_h|_E \in \mathbb{P}_2(E), \forall E \in \tau^h\},$$

where  $N_h = \dim P_h = 2N_{el} + 1$ . We can express the fully-discrete solution  $X_h^{k+1,n}$  as

$$X_h^{k+1,n} = \sum_{j=1}^{N_h} \xi_{h,j}^{k+1,n} \psi_j.$$

Substituting into (21), we obtain the system of equations

$$(M + \Delta t K) \xi_h^{k+1,n} = M \xi_h^{k+1,n-1} + \Delta t G_h^{k,n}, \tag{25}$$

where  $M_{ij} = (\psi_j, \psi_i)_{(L^2)^3}$ ,  $K_{ij} = (A_0^{-1} B_0 \psi_{j,z}, \psi_{i,z})_{(L^2)^3}$  and  $G_h^{k,n} = g(t_n, X_h^{k,n}, \psi_i)$ .

Let  $\alpha^n$ ,  $\beta^{k,n}$  and  $\gamma^{k,n}$  be the solution vectors for velocity, temperature and volume fraction. Given that  $\xi_h^{k,n} = \begin{bmatrix} \alpha^n \\ \beta^{k,n} \\ \gamma^{k,n} \end{bmatrix}$ , we solve the fixed-point equation (25) iteratively using the mathematical software MATLAB with stopping criterion

$$\frac{\|\beta^{k+1} - \beta^k\|_{fro}^2 + \|\gamma^{k+1} - \gamma^k\|_{fro}^2}{\|\beta^{k+1}\|_{fro}^2 + \|\gamma^{k+1}\|_{fro}^2} < 10^{-12},$$

where  $\beta^k$ ,  $\gamma^k$  are  $(2N_{el} + 1) \times N$  matrices with columns  $\beta^{k,n}$ ,  $\gamma^{k,n}$  for each  $n = 1, 2, \dots, N$  and  $\|\cdot\|_{fro}$  is the Frobenius norm. The obtained numerical results for the velocity, temperature and volume fraction are presented in graphical and tabular form as shown in Figures 1 to 6 and Tables 1 to 2.

Figures 1 to 3 show plots of the velocity, temperature, and volume fraction approximations over time for different values of  $N = N_t$ . We observe that for each  $N_t$ , the temperature and the volume fraction increase over time. Moreover, for each  $N_t$ , the velocity approaches a periodic steady state as time increases. Figures 4 to 6 show profiles of the velocity, temperature, and volume fraction approximations for different values of  $N_{el}$ . The velocity and temperature plots in Figures 4 and 5 (respectively) are almost indistinguishable from each other, implying that only a small number of elements are required to achieve a reasonable approximation. However, this was not the case for the volume fraction (Figure 6); a significantly larger number of elements are required in order to obtain a reasonable approximation.

In Table 1, the  $L^2$ -error  $e_h^N(\Delta t) = \|X_h^N - X(t_N)\|_{(L^2)^3}$  at time  $t_N = \bar{t}$  is shown for different values of the spatial mesh parameter  $h$  when  $\Delta t = \bar{t}/20$ . The spatial mesh convergence rate is estimated using the computed value of  $e_h^N(\Delta t)$  and compared with the theoretical results obtained in Corollary 2. The weak solution  $X(t_N)$  is represented by the fully-discrete solution on a fine mesh with  $h = 0.01$  and  $\Delta t = \bar{t}/2000$ . From Table 1, as  $h$  decreases the error decreases and the spatial convergence rate increases towards a value of 3. These computed values indicate a cubic rate of convergence in  $h$  and is consistent with the theoretical results obtained in Section 5 for the case of quadratic elements ( $m = 2$ ). Furthermore, the

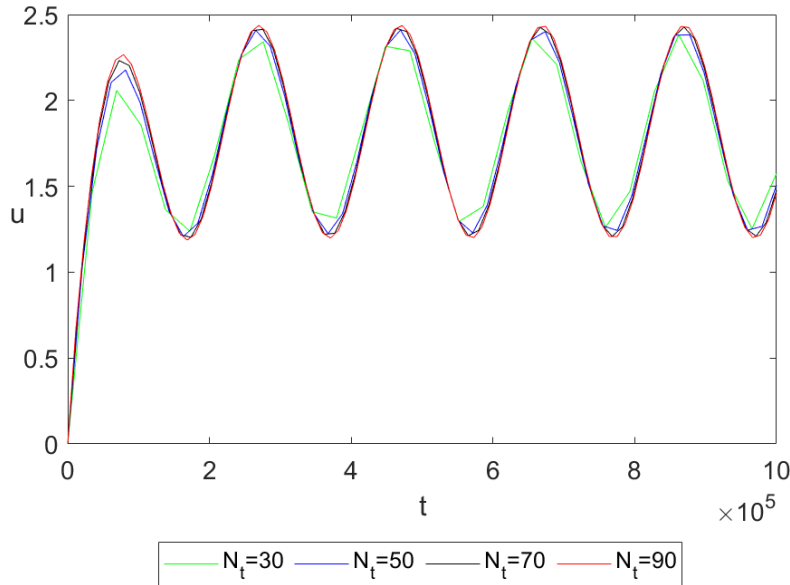


**Fig. 1:** Plots of  $u$  vs.  $t$  for Varying  $N_t$  with  $N_{el} = 50$  and  $z = 0.5$ .

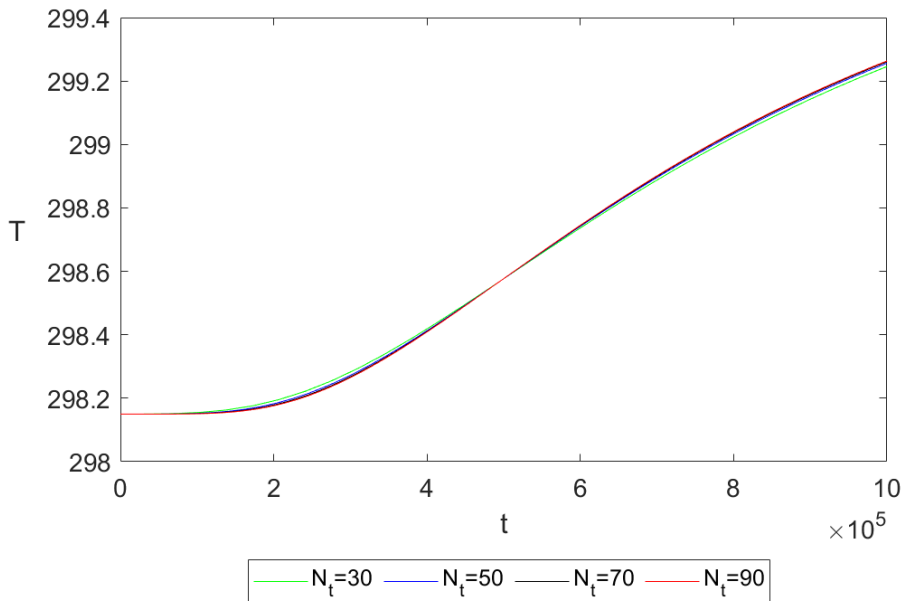


**Fig. 2:** Plots of  $T$  vs.  $t$  for varying  $N_t$  with  $N_{el} = 50$  and  $z = 0.5$ .

computed cubic convergence rate is consistent with experimental order of convergence results obtained by Bänsch and Morin [16] for piecewise quadratic finite element approximations.

Table 2 displays the  $L^2$ -error  $e_h^N(\Delta t)$  at time  $t_N = \bar{t}$  for different values of the time step-size  $\Delta t$  when  $h = 0.2$ . The temporal mesh convergence rate is estimated using the computed  $L^2$ -error and a comparison is made with the theoretical rate obtained in Corollary 2. From Table 2, we can observe that the error decreases as  $\Delta t$  decreases; this reduction in error is less pronounced than in Table 1. Furthermore, the convergence rate increases towards unity with decreasing  $\Delta t$ , which is consistent with the theoretical results on the fully-discrete solution in Section 5. The computed linear rate of convergence

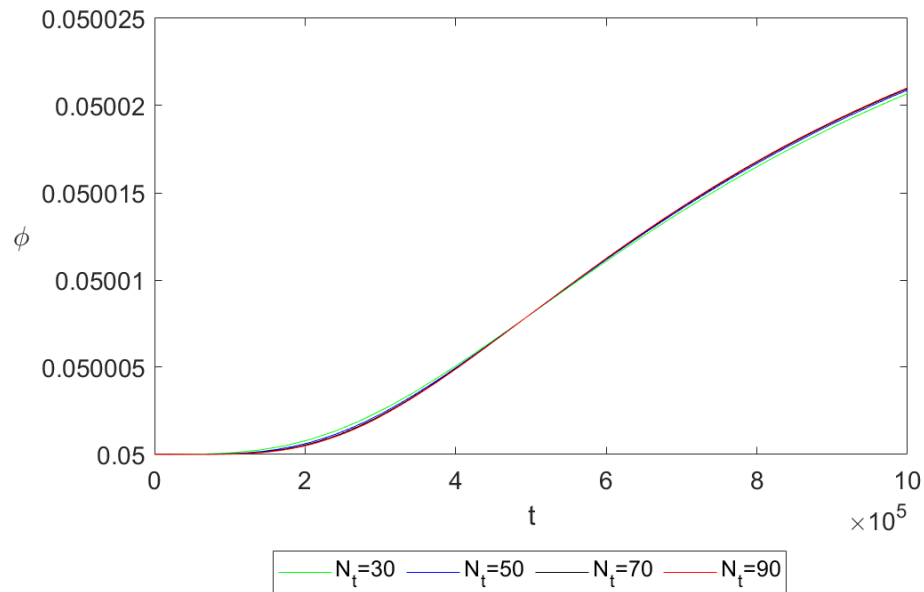


**Fig. 3:** Plots of  $\phi$  vs.  $z$  for varying  $N_t$  with  $N_{el}=50$  and  $z=0.5$ .

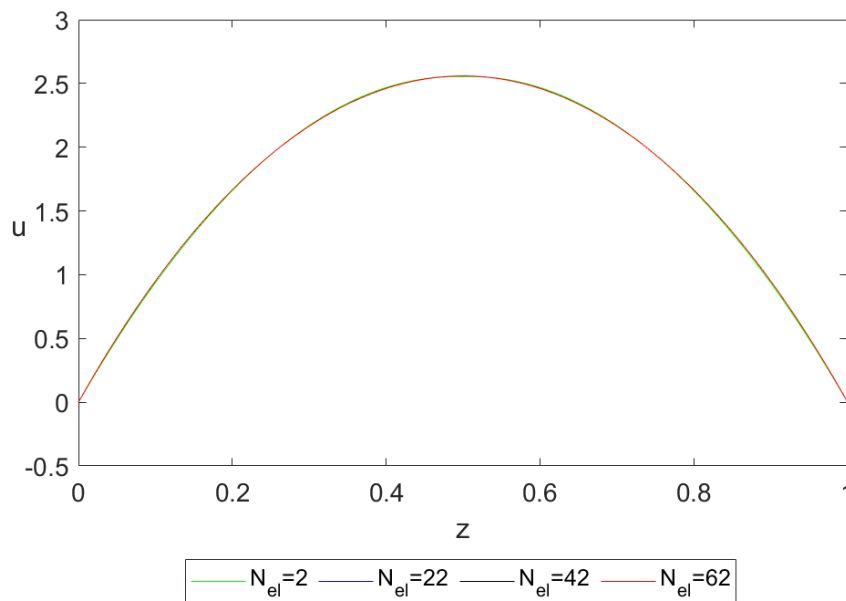


**Fig. 4:** Plots of  $u$  vs.  $z$  for varying  $N_{el}$  with  $N_t = 100$  and  $\bar{t} = 10^6$ .

in  $\Delta t$  arises from the Backward-Euler scheme used for the time discretization, and is consistent with theoretical and computational results obtained for time-dependent fluid flow problems investigated in Jia et al. [8].

### 7 Conclusion

In this article, we analyzed the Galerkin finite element method for an unsteady two-phase Poiseuille nanofluid flow and heat transfer based on the Buongiorno model. The high degree of non-linearity in the governing equations (particularly the temperature and volume fraction) proved to be the main difficulty in the finite element analysis. Using the fixed-point

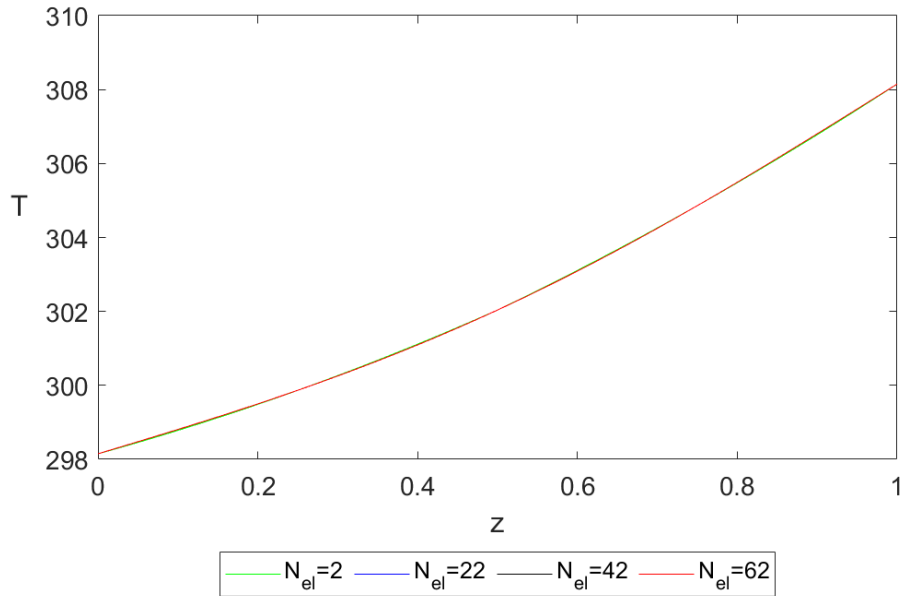


**Fig. 5:** Plots of  $T$  vs.  $z$  for varying  $N_{el}$  with  $N_t = 100$  and  $\bar{t} = 10^6$ .

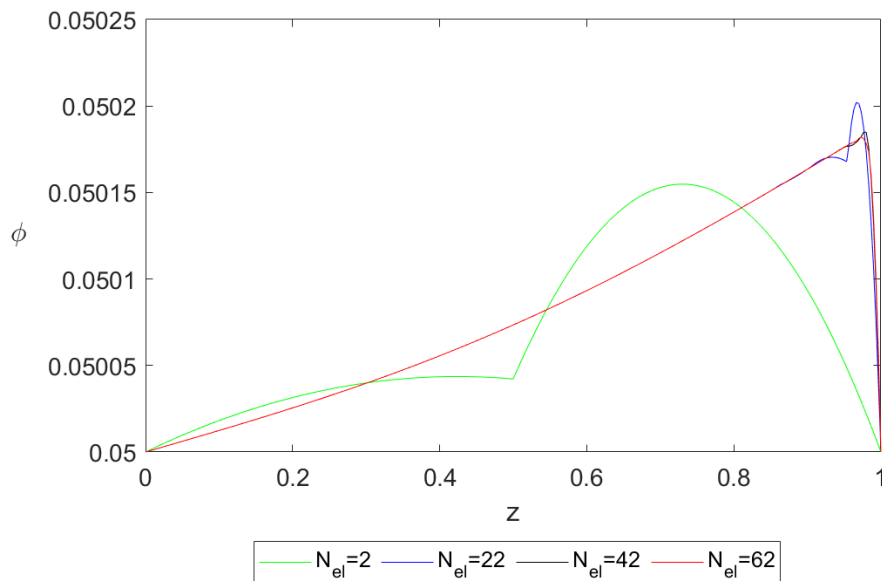


**Fig. 6:** Plots of  $\phi$  vs.  $z$  for varying  $N_{el}$  with  $N_t = 100$  and  $\bar{t} = 10^6$ .

iteration method when dealing with the non-linearities, we discussed the existence and uniqueness of the weak, semi-discrete and fully-discrete forms along with obtaining  $L^2$ -error estimates for the semi-discrete and fully-discrete forms. The numerical computations done for the spatial and temporal rates of convergence in Section 6 proved to be in accordance with the theoretical results from Section 5. This indicated that the Galerkin finite element method is suitable for solving Poiseuille nanofluid problems based on the Buongiorno model. We believe the present study is impactful since Poiseuille flow models play important roles in fluid dynamics and have many applications in the medical sciences. Moreover, this work contributes to providing theoretical support for applying the Galerkin finite element method to the model.

$h$	$e_h^N(\Delta t)$	Spatial Rate	Computational Time, sec
1/2	$5.2830 \times 10^{-2}$		3.88229
1/4	$6.8236 \times 10^{-3}$	2.9527	5.44585
1/6	$2.0391 \times 10^{-3}$	2.9789	7.07477
1/8	$3.0204 \times 10^{-4}$	2.9820	14.2058
1/10	$1.5514 \times 10^{-4}$	2.9856	16.5768

**Table 1:** Table Showing Mesh Parameter  $h$ , Absolute Error  $e_h^N(\Delta t)$ , Spatial Convergence Rate and Computational Time with  $\Delta t = \bar{t}/20$ .

$\Delta t$	$e_h^N(\Delta t)$	Temporal Rate	Computational Time, sec
$\bar{t}/30$	0.2583		16.6559
$\bar{t}/50$	0.1632	0.8751	29.1953
$\bar{t}/70$	0.1189	0.9251	38.6864
$\bar{t}/90$	0.0932	0.9586	53.5539
$\bar{t}/110$	0.0763	0.9843	60.3190

**Table 2:** Table Showing Time Step-size  $\Delta t$ , Absolute Error  $e_h^N(\Delta t)$ , Temporal Convergence Rate and Computational Time with  $h = 0.2$ .

## Declarations

**Competing interests:** None.

**Authors' contributions:**

Andrew O. McCartney: Formal analysis, Investigation, Methodology, Software, Writing - original draft, Writing - review & editing.

Victor M. Job: Conceptualization, Investigation, Methodology, Resources, Writing - review & editing.

**Funding:** None.

**Availability of data and materials:** No data was used for the research described in the article.

**Acknowledgments:** None.

## References

- [1] M.J. Turner, R.W. Clough, H.C. Martin, L.J. Topp. Stiffness and Deflection Analysis of Complex Structures *Journal of the Aeronautical Sciences* **23(9)** (1956), 805–823.
- [2] M. Wheeler. A Priori  $L_2$  Error Estimates for Galerkin Approximations to Parabolic Partial Differential Equations. *SIAM Journal on Numerical Analysis* **10(4)** (1973), 723–759.
- [3] Z. Weng, X. Feng, D. Liu. A Fully Discrete Stabilized Mixed Finite Element Method for Parabolic Problems. *Numerical Heat Transfer, Part A: Applications* **63(10)** (2013), 755–775.
- [4] B. Jin, R. Lazarov, J. Pasciak, Z. Zhou. Error Analysis of a Finite Element Method for the Space-Fractional Parabolic Equation. *SIAM Journal on Numerical Analysis* **52(5)** (2014), 2272–2294.
- [5] E. Burman, J. Ish-Horowicz, L. Oksanen. Fully Discrete Finite Element Data Assimilation Method for The Heat Equation. *ESAIM: Mathematical Modelling and Numerical Analysis* **52(5)** (2018), 2065–2082.
- [6] Y. Shang. New Stabilized Finite Element Method for Time-Dependent Incompressible Flow Problems. *International Journal for Numerical Methods in Fluids* **62** (2010), 166–187.
- [7] P. Huang, X. Feng, D. Liu. A Stabilized Finite Element Method for the Time-Dependent Stokes Equations Based On Crank-Nicolson Scheme. *Applied Mathematical Modelling* **37(4)** (2013) 1910–1919.
- [8] H. Jia, K. Li, S. Liu. Characteristic Stabilized Finite Element Method For The Transient NavierStokes Equations. *Computer Methods In Applied Mechanics And Engineering* **199(45-48)** (2010), 2996-3004.
- [9] X. Li, X. Yang, Y. Zhang. Error Estimates Of Mixed Finite Element Methods for Time-Fractional NavierStokes Equations. *Journal Of Scientific Computing* **70(2)** (2016), 500–515.
- [10] J. Buongiorno. Convective Transport In Nanofluids. *Journal Of Heat Transfer* **128(3)** (2006), 240–250.
- [11] S.Z. Alamri, R. Ellahi, N. Shehzad, A. Zeeshan. Convective Radiative Plane Poiseuille Flow Of Nanofluid Through Porous Medium With Slip: An Application Of Stefan Blowing. *Journal of Molecular Liquids* **273** (2019), 292–304.

- [12] M. Sheikholeslami, D.D. Ganji, M.M. Rashidi. Magnetic Field Effect On Unsteady Nanofluid Flow And Heat Transfer Using Buongiorno Model. *Journal of Magnetism And Magnetic Materials* **416** (2016), 164–173.
  - [13] Z. Boulahia, C. Boulahia, R. Sehaqui. Two-Phase Computation Of Free Convection And Entropy Generation Inside An Enclosure Filled By A Hybrid  $Al_2O_3-TiO_2$ -Cu water Nanofluid Having A Corrugated Heat Source Using The Generalized Buongiorno Mathematical Model: Employment of Finite Volume Method. *Materials Today:Proceedings* **30** (2020), 1056–1067.
  - [14] E. Bänsch. A Thermodynamically Consistent Model for Convective Transport in Nanofluids: Existence of Weak Solutions and FEM Computations. *Journal of Mathematical Analysis And Applications* **477(1)** (2019), 41-59.
  - [15] M.S. Anwar. Numerical Study of Transport Phenomena in a Nanofluid using Fractional Relaxation Times in Buongiorno Model. *Physica Scripta* **95(3)** (2020), 035211.
  - [16] E. Bänsch, P. Morin. Convective Transport in Nanofluids: Regularity of Solutions And Error Estimates for Finite Element Approximations. *Journal of Mathematical Fluid Mechanics* **23** (2021), 42.
  - [17] J. Lions, E. Magenes. *Non-Homogeneous Boundary Value Problems And Applications, 1st Ed.* Berlin Springer-Verlag, (1972).
  - [18] A. Ern, J. Guermond. *Theory And Practice Of Finite Elements, 1st Ed.* New York Springer, (2004).
  - [19] M. Braun. *Differential Equations And Their Applications, 3rd Ed.* New York Springer-Verlag, (1983).
  - [20] S. Brenner, L. Scott. *The Mathematical Theory Of Finite Element Methods, 3rd Ed.* New York Springer, (2008).
  - [21] I. Dinçer, C. Zamfirescu. *Drying Phenomena: Theory and Applications, 1st Ed.* Chichester Wiley & Sons Ltd, (2016).
  - [22] P. Auerkari. Mechanical and Physical Properties of Engineering Alumina Ceramics. *VTT Tiedotteita - Meddelanden - Research Notes* 1792 (1996).
-